Radiocarbon, Vol 59, Nr 6, 2017, p 1955–1967 DOI:10.1017/RDC.2017.120
Selected Papers from the 8th Radiocarbon & Archaeology Symposium, Edinburgh, UK, 27 June–1 July 2016

U/TH AND ^{14}C CROSSDATING OF PARIETAL CALCITE DEPOSITS: APPLICATION TO NERJA CAVE (ANDALUSIA, SPAIN) AND FUTURE PERSPECTIVES

Hélène Valladas[1*] • Edwige Pons-Branchu[1] • Jean Pascal Dumoulin[2] • Anita Quiles[3] • José L Sanchidrián[4] • Maria Ángeles Medina-Alcaide[5]

[1]Laboratoire des Sciences du Climat et de l'Environnement, LSCE/IPSL, CEA-CNRS-UVSQ, Université Paris-Saclay, Bâtiment 12, avenue de la terrasse, 91198 Gif Sur Yvette Cedex, France.
[2]Laboratoire de Mesure du Carbone 14 (LMC14), LSCE/IPSL, CEA-CNRS-UVSQ, Université Paris Saclay, F-91191 Gif-sur-Yvette, France.
[3]Institut Français d'Archéologie Orientale, Pôle archéométrie, 37 rue al-Cheikh Aly Youssef, B.P. Qasr el-Ayni, 11652, 11441 Le Caire, Egypt.
[4]University of Cordoba UCO, Geography and Territory Sciences, Cardenal Salazar s/n, 14071 Cordoba, Spain.
[5]University of the Basque Country UPV/EHU, Geography, Prehistory and Archaeology, Tomás y Valiente s/n, 01006 Vitoria-Gasteiz, Spain.

ABSTRACT. ^{14}C and U/Th methods were used to date three thin carbonate layers deposited on decorated walls of Nerja Cave (Malaga, southern Spain) in order to constrain the age of the parietal non-figurative marks situated under these carbonate layers. Modern formations were also dated to estimate the detritic contribution for the U/Th method and the dead carbon proportion for ^{14}C dating. We sampled two locations with ocher painting marks. In one case (mark 1), the good agreement between the ages obtained by the two methods suggests that the sample was not subjected to post-deposition alteration and that the results are reliable. In the other case (mark 2), the age discrepancy between the two methods reached 30,000 yr, indicating that geochemical alteration had affected the sample and that one or both results were inaccurate. The ages for mark 1 indicate that this type of non-figurative representation is older than 25,000 cal BP and that it can be associated with the oldest attested Paleolithic occupation of Nerja Cave.

KEYWORDS: crossdating, Nerja Cave, parietal carbonate, radiocarbon, U/Th.

INTRODUCTION

Nerja Cave (Nerja, Malaga, southern Spain), discovered in 1959, is a large cavity (surface of ca. 35,484 m^2 and length of ca. 4843 m) located in the southern part of the Iberian Peninsula. Between 1960 and 1987 excavations in the outer galleries revealed a long Upper Palaeolithic sequence including layers attributed to the Gravettian, the Solutrean, and the Magdalenian cultures. Numerous archaeological materials such as flints, bones, ocher fragments, and charred plant remains were found on the floor of the inner galleries. These galleries contain many examples of parietal art: 32 figurative motifs (horses, deer, ibex, and undefined quadrupeds), 254 signs and 263 stained speleothems (Sanchidrián 1994, 1997, 2001). Radiocarbon (^{14}C) analyses were done on archaeological samples found during excavations to establish the periods of human occupation within the cave (Jordá and Aura 2008, 2009) but in the absence of direct dating, the chronology of the parietal art still remains problematic since the majority of Palaeolithic paintings were made with red pigment, especially the graphics located in the inner galleries.

Scientific investigations have been carried out since 2008 by Sanchidrián and his team to study the periods of Palaeolithic occupation of the inner galleries and to connect them with the chronology of the parietal art and the geomorphological evolution of the cave. In 2012, a research program was run by Cordoba University and the *Fundación Cueva de Nerja*, in collaboration with the Laboratoire des Sciences du Climat et de l'Environnement, to develop protocols to date the parietal representations (Quilès et al. 2014). At present, a thin

*Corresponding author. Email: helene.valladas@lsce.ipsl.fr.

secondary carbonate deposit covers part of them. Therefore the age of these overlying formations is assumed to provide a minimum age (*terminus ante quem*) for the underlying representations.

Since the 2000s, the uranium-thorium (or $^{230}Th/^{234}U$) method has been used to date thin calcite layers deposited on decorated walls in order to constrain the age of the parietal representations situated below or above these calcite layers. The method was first applied to the Covalanas Cave, Spain (Bischoff et al. 2003) and to the Creswell Cave in the United Kingdom (Pike et al. 2005) where calcite deposits covered parietal engravings. Then, in 2012, $^{230}Th/^{234}U$ ages obtained on ca. 50 parietal representations of 11 Palaeolithic Spanish caves were published by Pike et al. However, in most cases it was only possible to make one $^{230}Th/^{234}U$ analysis per representation and the results obtained remain uncertain because of the impossibility of assessing their reliability by showing that the dated calcite samples did not undergo diagenetic processes and behave as a closed system (Clottes 2012; Pike et al. 2012; Pons-Branchu et al. 2014a). For this reason, Hoffmann et al. (2016) therefore proposed to check the relevance of the $^{230}Th/^{234}U$ ages by dating several subsamples along the growth axis of the calcite deposit. Assuming that leaching cannot affect all calcite sublayers, obtaining $^{230}Th/^{234}U$ ages in stratigraphic order would confirm the closed system behavior. This approach, applied to two Spanish caves (La Pasiega and Fuente del Trucho), provided coherent results that are in agreement with the results previously obtained by Pike et al. (2012) for the same paintings. A similar approach was used by Aubert et al. (2007, 2014) who performed analyses on several carbonate layers located on either side of parietal decorations present in Asian caves (Timor and Sulawesi). This stratigraphic control makes it possible to test the coherence of the results and to constrain the ages of the representations.

However, as many calcite layers are too thin for several $^{230}Th/^{234}U$ analyses to be performed across their growth axis, some researchers have proposed to perform crossdating by using $^{230}Th/^{234}U$ and ^{14}C methods on the same parietal $CaCO_3$ sample to compare the results and to check that the sample behaved as a "closed" system (Plagnes et al. 2003; Fontugne et al. 2013; Pons-Branchu et al. 2014a; Shao et al. 2017). For example, these two methods applied on a calcite deposit in the cave of Gua Saleh (Borneo) yielded compatible or rather different results depending on the samples and thus this comparison showed that in some cases the sample behaved as a geochemically open system and yielded erroneous $^{230}Th/^{234}U$ ages (Plagnes et al. 2003).

This approach based on $^{230}Th/^{234}U$ combined with ^{14}C analyses enables the results obtained on the same sample by the two methods to be compared and can thus be very useful to highlight possible post-deposition diagenetic processes leading to a geochemically open system and erroneous ages. It can be inferred that agreement between the two results suggests a closed system behavior of the dated sample and that the dates obtained are reliable, whereas disagreement between them should indicate that geochemical alteration has affected the sample and that one or both results are inaccurate. This crossdating approach was tested in Nerja Cave on secondary carbonate samples deposited on two parietal red marks. We also discuss the validity of the correction to be applied on each method, i.e. detrital correction for the $^{230}Th/^{234}U$ method, and dead carbon correction for the ^{14}C method.

SAMPLES AND METHODS

Two red marks that are clearly of anthropic origin were selected because they were in the same area (Figure 1) and were overlain by a secondary carbonate deposit. These types of red signs

https://doi.org/10.1017/RDC.2017.120 Published online by Cambridge University Press

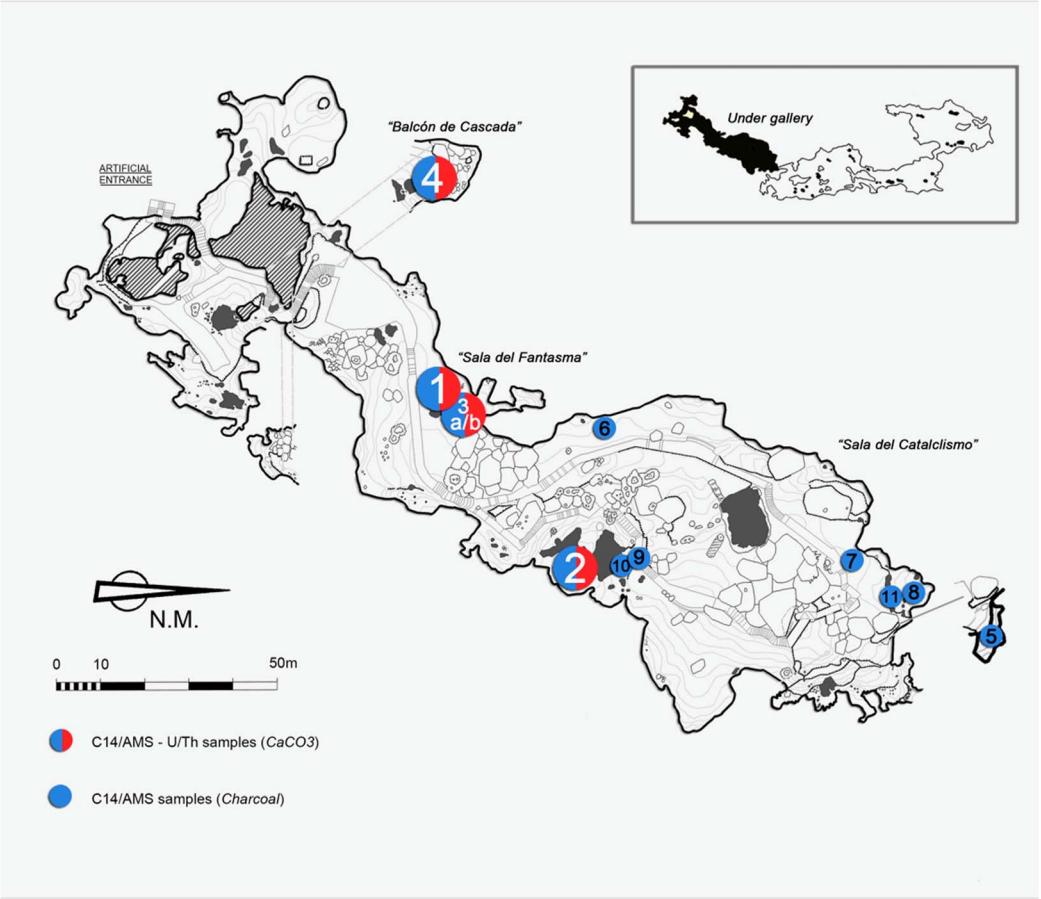

Figure 1 Locations of the dated samples in the upper galleries: dots 1 and 2 are modern $CaCO_3$ deposits (GN12-29 and GN12-24); dots 3 and 4 are $CaCO_3$ deposited on mark 2 (samples GN12-25 and GN12-27) and on mark 1 (sample GN14-17); and dots 5–11 are charcoal samples whose ^{14}C results are discussed in the article (Sanchidrian 1994, 1997).

that are not figurative graphical symbols are commonly found in prehistoric caves but their meaning remains unknown (Medina-Alcaide et al. 2017).

- Mark 1 is an ensemble of three aligned red dots measuring 2 × 1.5 cm, drawn with ocher on a speleothem. The support matches with the edge of the calcite draperies located at a height of 160 cm. The dots are partially overlain by a thin secondary carbonate deposit (Figure 2).
- Mark 2 is composed of large red spots located in a stalagmitic flowstone at a height of 130 cm (Figure 3). The spots are also partially overlain by two thin superposed secondary calcareous deposits.

Sampling

Small fragments (a few mm^2 to ca. 1 cm^2) of the $CaCO_3$ layers overlying the red marks 1 (GN sample GN14-17) and 2 (GN12-25 and GN12-27 samples) were carefully sampled with a scalpel as close as possible to the marks, without causing any visible deterioration. GN12-25

https://doi.org/10.1017/RDC.2017.120 Published online by Cambridge University Press

Figure 2 Picture of mark 1 with localization of the sampled point (GN14-17), in the area of the *Balcon de Cascada en galerias Bajas*.

and GN12-27 samples originating from two different layers (yellow and gray, respectively) are in stratigraphic order: the deepest sample GN12-25 is situated just above the red mark 2 and below GN12-27 (see Figure 3).

Their stratigraphic relation with the painting was carefully verified and pictures were taken throughout the sampling process to record the exact location of the samples. Each sample was divided into two aliquots for $^{230}Th/^{234}U$ and ^{14}C dating. For the largest sample (GN12-27), it was possible to perform three replicate $^{230}Th/^{234}U$ analyses on three aliquots (GN12-27a, b and c), taken one next to the other in the same layer. In order to constrain the detrital fraction content for $^{230}Th/^{234}U$ dating, two recent/modern $CaCO_3$ samples were also collected. The first was a still active soda straw (GN12-29), previously analyzed for ^{14}C dating (Sanchidrián et al. 2017) and the second (GN12-24) was a very recent deposit that grew on a bowl placed below water dripping from the roof.

Dating Analyses

^{14}C Dating

The three aliquots of carbonate samples (solid fragments of GN14-17, GN 2-25, and GN12-27) were prepared according to the protocol described by (Tisnérat-Laborde et al. 2001). First, they were cleaned using an ultrasound bath in distilled water, then gently attacked for 3 min in nitric acid (0.01N) and finally rinsed again in distilled water. The calcite was reacted with phosphoric

https://doi.org/10.1017/RDC.2017.120 Published online by Cambridge University Press

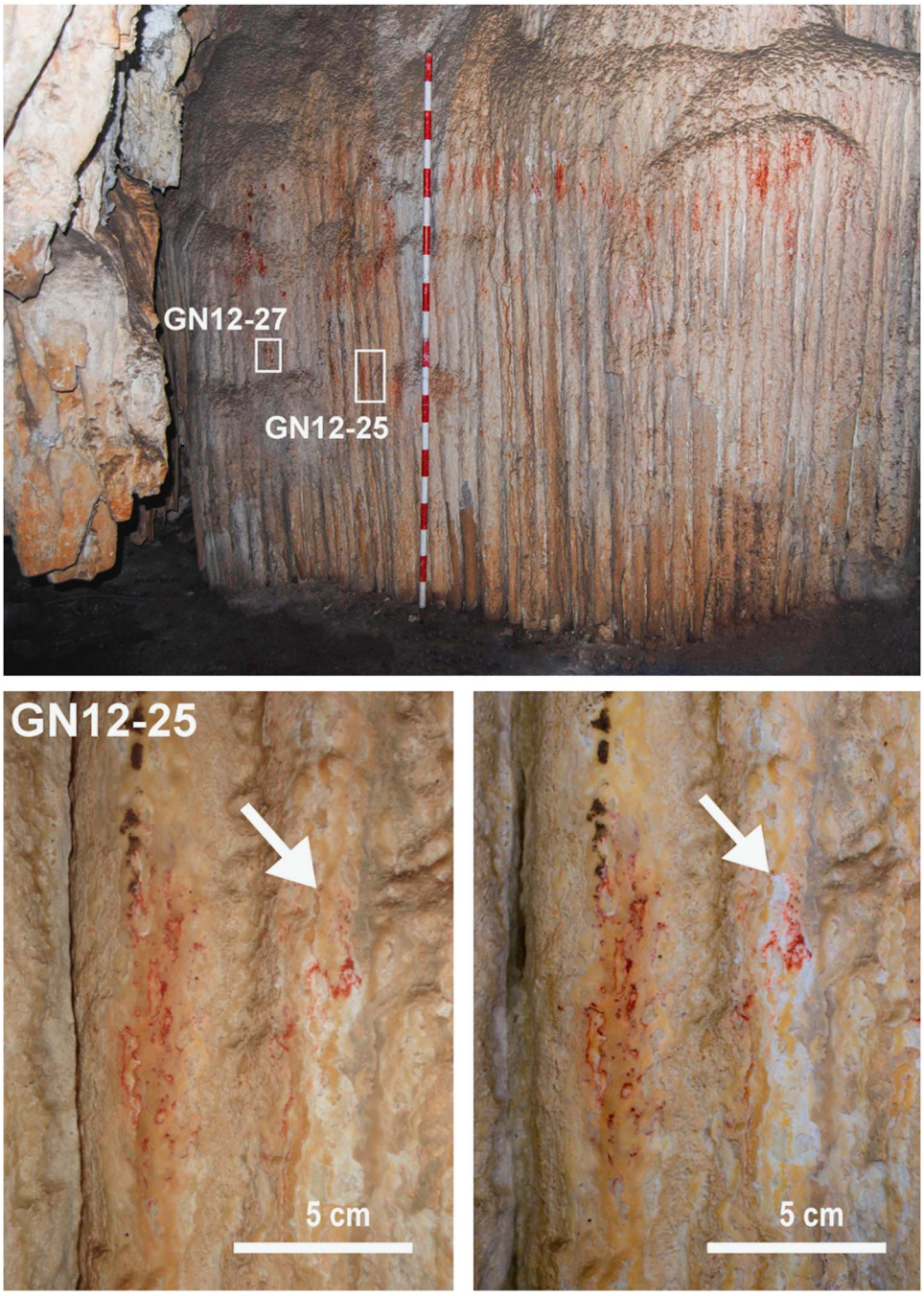

Figure 3 Picture of mark 2 with localization of the two sampled points (GN12-25 and GN12-27), in the area of *Sala del Fantasma*. The two samples are 40 cm apart. The lowest part of the figure shows the wall before and after the sampling of GN12-25.

https://doi.org/10.1017/RDC.2017.120 Published online by Cambridge University Press

acid under vacuum and the CO_2 produced was converted to graphite then measured using the accelerator mass spectrometer of the LMC14 (Artemis, CEA Saclay; Cottereau et al. 2007).

^{14}C measurements were first corrected according to the ^{13}C values measured by the Artemis facility and for the background contribution, the ages were calculated following Mook and van der Plicht (1999).

$^{230}Th/^{234}U$ Dating

U and Th analyses were performed on GN12-25, GN12-27a, b, c, GN14-17 and on the modern samples (GN12-29 and GN12-24). U-Th separation and purification were performed at LSCE following a procedure described in Pons-Branchu et al. (2014b). Between ca. 50 and 125 mg of sample was dissolved with diluted HCl in a Teflon beaker and mixed with a triple ^{229}Th ^{233}U ^{236}U spike. U and Th were co-precipitated with $Fe(OH)_3$. U-Th separation and purification were performed on a 0.5-mL column filled with U-TEVA and a small amount of pre-filter resin at the bottom of the column. The $CaCO_3$ matrix and trace elements were eluted in 3N HNO_3, while the Th fraction was eluted using 3N HCl and the U fraction using 1N HCl. The U and Th isotopic analyses were performed on a Neptune Plus multi-collector inductively coupled plasma mass spectrometer (MC-ICP-MS) fitted with a jet pump interface. For mass fractionation corrections of isotopic ratios, we used an exponential mass fractionation law (normalized to natural $^{238}U/^{235}U$ isotopic ratio) and standard/sample bracketing (using a mixture of our triple spike and Hu-1 uraninite). For more details on the analytical procedure, see Pons-Branchu et al. (2014b).

After corrections for peak tailing, hydrate interference and chemical blanks, age calculations from the isotopic data were carried out based on iterative age estimation.

RESULTS

^{14}C Dating

The ^{14}C ages of the $CaCO_3$ specimens were corrected for dead carbon contents (called dead carbon proportion or dcp) assuming five percentage values (respectively 0, 5, 10, 20, and 50%) that cover the range of possible dcp values in speleothems. Typical dcp values range between 5 to 15%. The corrected values were then calibrated (Table 1) using the IntCal13 calibration curve (Reimer et al. 2013). For the samples GN14-17, GN12-25, and GN12-27, the corrected calibrated age ranged respectively between 25,374 and 18,430 cal yr BP, between 33,769 and 27,491 cal yr BP and between 17,024 and 9142 cal yr BP, depending on the dead carbon proportion considered (0, 5, 10, 20, and 50%). Sample GN12-29 (a soda straw) displayed a modern age.

$^{230}Th/^{234}U$ Results

Uranium content varied between 19.60 ± 0.04 and 1.40 ± 0.001 ppm. The isotopic composition of uranium was relatively close to equilibrium, with $\delta\ ^{234}Ui$ between 31.5 ± 0.6 and -14.7 ± 1.2‰. The ^{232}Th content ranged between 78.05 ± 0.10 and 4.08 ± 0.01 ppb; the $^{230}Th/^{232}Th$ ratio varied between 5.16 ± 0.14 and 68.93 ± 0.18, indicating that a proportion of ^{230}Th originated from the detrital fraction was present at the time of the speleothem formation.

A correction for the detrital fraction assuming a $^{230}Th/^{232}Th$ initial ($^{230}Th/^{232}Th_0$) value of $1.25 \pm 50\%$ was applied to calculate the corrected ages. Another correction was applied using the measured $^{230}Th/^{232}Th_0$ of the present day $CaCO_3$ precipitated within the bowl (equal to

https://doi.org/10.1017/RDC.2017.120 Published online by Cambridge University Press

Table 1 Results of ^{14}C analyses performed on three carbonate deposits sampled respectively on mark 1 (GN14-17), mark 2 (GN 12-25 and GN 12-27) and on a still active soda straw (GN12-29; *from Sanchidrián et al. 2017).

Ref. on map (Figure 1)	Lab code	Sample nr	Percent modern carbon (%)		^{14}C BP age		Calibrated interval range cal BP–0% dcp	Calibrated interval range cal BP–5% dcp	Calibrated interval range cal BP–10% dcp	Calibrated interval range cal BP–20% dcp	Calibrated interval range cal BP–50% dcp
1	SacA 34253*	GN12-29*	97.73	0.31	185	30	300, modern	Modern	Modern	Modern	Out of range
3a	SacA 34251	GN12-25	2.67	0.07	29,110	200	33,769–32,821	33,476–32,108	32,648–31,469	31,496– 31,030	27,860–27,491
3b	SacA 34252	GN12-27	17.81	0.13	13,860	60	17,024–16,522	16,431–15999	15,786–15,323	14,068–13,769	9,426– 9,142
4	GifA15552 SacA 43953	GN14-17	7.46	0.08	20,850	30	25,374–25,002	25,018–24,351	24,300–23,819	23,301– 22,716	18,709– 18,430

Table 2 Uranium and thorium contents, isotopic ratios and ages.

Ref. on map (Figure 1)	Sample	^{238}U (ppm)		^{232}Th (ppb)		$\delta^{234}U_M$ (‰)		$^{230}Th/^{238}U$		$^{230}Th/^{232}Th$		Age (yr BP)		$\delta^{234}U_T$ (‰)		Cor. age* yr BP, error		Cor. age** yr BP/*yr AD*, error	
1	GN12-29	19.600	0.043	11.73	0.12	31.5	0.6	0.0048	0.0001	24.70	0.41	446	9	31.5	0.6	415	± 25	339	*15*
2	GN12-24	1.398	0.001	4.08	0.01	–6.0	1.09	0.005	0.0001	5.16	0.14	475	15	–6.0	1.1	475	15	*1992*	22
4	GN14-17	4.454	0.002	42.36	0.06	–14.9	1.1	0.2160	0.0006	68.93	0.18	26982	113	–16	1.1	26462	371	25189	212
3a	GN12-25	1.489	0.0004	56.54	0.16	12.5	1.0	0.4400	0.0016	38.18	0.14	62113	394	14.7	1.2	60276	1300	55848	716
3b	GN12-27 a	1.712	0.001	56.60	0.216	13.82	0.85	0.2547	0.0015	25.35	0.15	31500	243	14.87	0.92	29899	1037	26024	534
3b	GN12-27 b	2.319	0.001	78.05	0.142	1.33	1.83	0.2700	0.0013	25.41	0.12	34174	276	1.44	1.98	32460	1122	28321	579
3b	GN12-27 c	2.158	0.001	44.81	0.121	8.86	0.64	0.2513	0.001	38.31	0.14	31200	160	9.58	0.69	30144	685	27572	358

$^{238}U/^{230}Th$, $^{234}U/^{238}U$ (expressed as $\delta^{234}U$), and $^{230}Th/^{232}Th$ activity ratios are reported.

$\delta^{234}U = (\{^{234}U/^{238}U\}meas/\{^{234}U/^{238}U\}equilibrium - 1) \times 1000$ with $^{234}U/^{238}Uequilibrium = 54.97 \times 10^{-6}$ (molar ratio, Cheng et al. 2013). The ages are expressed as yr BP (before 1950).

*Corrected ages using $^{230}Th/^{232}Th_0$ activity ratio of $1.25 \pm 50\%$.

**Corrected ages using $^{230}Th/^{232}Th_0$ activity ratio of 5.2 ± 0.3.

5.2 and with a double error bar at ± 0.3), because the age of this sample (GN12-24) is known to be less than 10 yr. This higher correction results in younger ages (see Table 2). The different analysis of the youngest layer covering mark 2 (Gn12-27a, b, and c) displayed a slight variability in uranium content, uranium isotopic composition and age.

DISCUSSION

Chronology

^{14}C and $^{230}Th/^{234}U$ Ages

^{14}C age determination of thin calcareous layers in karstic environments is hampered by the dcp that leads to an overestimation of the real age. This dead carbon results from soil (with old carbon) or host rock carbon (with no ^{14}C); see for instance Gascoyne and Nelson (1983), Goslar et al. (2000), and Genty et al. (2001). Previous ^{14}C analysis of the active soda straw (GN12-29) of Nerja Cave indicated a very small amount of dead carbon (less than 10%) for at least the recent period (Sanchidrián et al. 2017). Comparison between $^{230}Th/^{234}U$ and ^{14}C ages obtained on GN12-29 confirmed this suggestion for the modern period. As underlined by Tuccimei et al. (2011), a very low fraction of dead carbon indicates limited interaction between water percolating through the epikarst and host rock and a short time transit of the water. However, dcp content can vary in time and space by a few percent, in relation with hydrological changes within the cave (e.g. Griffiths et al. 2012; Noronha et al. 2014).

The GN14-17 sample shows a good agreement between the $^{230}Th/^{234}U$ ages (25,189 ± 212 yr BP) and the ^{14}C calibrated result (25,374–25,002 cal yr BP) assuming 0% dcp. This agreement suggests a closed system evolution and validates the results of the two methods and the small amount of dcp assumed at Nerja Cave. Therefore the ages deduced for the carbonate sample GN14-17 can be considered as a reliable *terminus ante quem* (i.e. minimum age) for the underlying red marking.

In the case of GN12-25 and GN12-27, the two methods yield results which are in agreement with their stratigraphic position: the age obtained on the deepest sample, GN12-25, is greater than the ages of GN12-27 which is located just above. However very different $^{230}Th/^{234}U$ and ^{14}C ages are obtained for these two samples. In the case of GN12-25, the $^{230}Th/^{234}U$ method yields 60,276 ± 1300 yr BP while the calibrated ^{14}C result, significantly younger, ranges between 33,770 and 27,491 cal yr BP depending on the considered dcp (0 to 50%). For the aliquot samples GN12-27a, b, c, the $^{230}Th/^{234}U$ ages are consistent and fall in the same time range, between 26,024 ± 534 and 28,321 ± 579 but the ^{14}C gives younger ages, from 17,024 to 9142 cal yr BP depending on the dcp. Therefore for these samples, the two methods yield divergent results, with $^{230}Th/^{234}U$ ages greater than ^{14}C ages (whatever the dcp taken into account). This age difference which reaches ca. 30,000 yr for the oldest sample (GN12-25) and ca. 10,000 for the youngest one (GN12-27) could be explained by two processes affecting the dated samples: the first one is an open system behavior of the carbonate layer with exchange of chemical elements (uranium, thorium, or carbon) between the $CaCO_3$ layer and seepage water or atmosphere; the second one is the incorporation of a small amount of the host rock in the dated carbonates (Fontugne et al. 2013).

An open system behavior of secondary carbonate deposits is expected to lead to uranium leaching due to its higher solubility than that of thorium. This phenomenon, previously observed in both massive speleothems and thin $CaCO_3$ deposits (see for example Borsato et al. 2003 or Plagnes et al. 2003), produces $^{230}Th/^{234}U$ apparent ages older than the true ones. Thorium addition (^{230}Th alone or via addition of a detrital component with a very high $^{230}Th/^{232}Th$ ratio) is also a possibility in the case of an open system and has already been proposed for some alpine

https://doi.org/10.1017/RDC.2017.120 Published online by Cambridge University Press

speleothems (Borsato et al. 2003). The addition of a ^{230}Th-rich detrital phase (for instance by dust particles) could not explain the age discrepancy obtained by the two methods for GN 12-17; indeed, the ^{230}Th/^{234}U ages of the three coeval samples are in close agreement but display, however, different ^{232}Th content and ^{230}Th/^{232}Th ratios. An open system behavior could also affect ^{14}C age determination by replacing intrinsic old carbon by cave atmospheric CO_2 at the time of alteration, leading to apparent ^{14}C ages younger than the true ones (e.g. Holmgren et al. 1994; Goslar et al. 2000; Bruthans et al. 2012; Roy-Barman and Pons-Branchu 2016). Thus, the effect of the opening of the system is expected to be different for the two chronometers.

On the other hand, the incorporation of a small amount of host rock within the sample could bias both ^{14}C and ^{230}Th/^{234}U toward apparent ages older than the real ones. For a 25,000-yr-old secondary deposit that contains the same amount of U as the host rock and a ^{234}U/^{238}U activity ratio close to 1, 1% of host rock contamination (older than 1,000,000 yr) results in a ^{230}Th/^{234}U age overestimated by ca. 1000 yr whereas 10% of host rock contamination leads to a ^{230}Th/^{234}U age overestimated by ca. 10,000 yr. The same amounts (1% and 10%) of host rock in the 25,000-yr-old carbonate sample will make the calibrated ^{14}C age older by ca. 50–100 yr and ca. 1000 yr, respectively. The impact of contamination for different amounts of host rock on the age of a 25,000-yr-old secondary carbonate sample is presented in Figure 4. In order to explain the discrepancy between ^{14}C and ^{230}Th/^{234}U ages, the amount of contamination by the host rock would have to be as high as 30%, assuming the same amount of uranium within the host rock and the secondary $CaCO_3$ layer. Such a process appears to be rather unlikely in the Nerja case, and therefore an open geochemical system with uranium leaching is a more probable explanation of the age difference between the two dating methods for the GN12-25 (and GN12-27) samples. Further investigations are necessary to show evidence of such a process before dating.

Implication for Rock Art Dating Methodology Using $CaCO_3$ Layers

During this study, the application of the ^{14}C and ^{230}Th/^{234}U chronometers to $CaCO_3$ thin layers demonstrated that the concomitant use of these two methods makes it possible to validate the ages obtained when the two methods give coherent results, and to invalidate them when the discrepancy cannot be explained by the incorporation of dead carbon (open system or

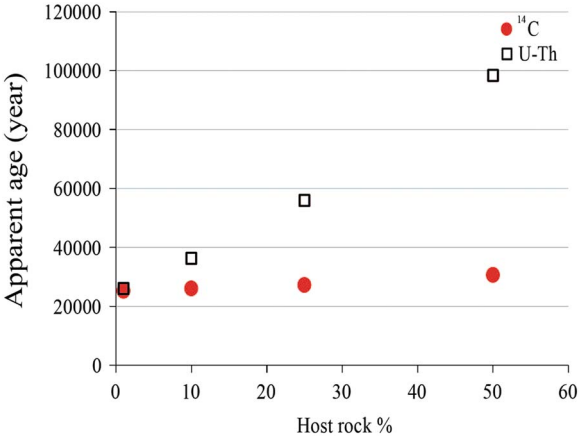

Figure 4 Effect of different percentages of host rock contamination on the ^{14}C and U/Th ages of a ca. 25,000-yr-old secondary thin layer.

https://doi.org/10.1017/RDC.2017.120 Published online by Cambridge University Press

contamination with host rock). This approach previously applied in different archaeological contexts proved to be very useful to discuss the validity of the results (e.g. Plagnes et al. 2003; Fontugne et al. 2013; Shao et al. 2017). The present study provides further support for generalizing the use of several dating methods whenever possible. ^{14}C and $^{230}Th/^{234}U$ are not the only methods applicable for dating such samples, and in certain cases, the $^{226}Ra/^{238}U$ or $^{231}Pa/^{235}U$ chronometers can also be successfully applied (Edwards et al. 1997; Pons-Branchu et al. 2005).

Speleothem Growth during Glacial Time

Speleothem deposition is controlled by climatic and environmental factors such as water availability, pCO_2 in the soil, dissolved calcium concentration and drip rate. Dry and/or ice cover periods are generally characterized by a lack of deposition due to slower water infiltration and to a lower CO_2 supply from vegetation and soil. Speleothem growth cessation has been observed in northern Europe during the coldest phases of the last glacial periods (Gordon et al. 1989; Baker et al. 1993; Pons-Branchu et al. 2010), whereas southern European and circum-Mediterranean regions are characterized by speleothem growth during the last glacial period, suggesting that this period was relatively humid (Kaufman et al. 1998; Bar-Matthews et al. 2003; Siddall et al. 2008; Fleitmann and Matte 2009; Moreno et al. 2010). GN14-17 was deposited during the maximum of the last glacial period (marine isotope stage 2). Therefore our results show that during MIS2 the climatic conditions in the Nerja area were humid enough to permit the formation of a thin calcite layer, at least for a short period. This result is in agreement with the climate reconstruction of central and southern Spain that evidenced a cold but humid period between 29 and 25 kyr BP (Domınguez-Villar et al. 2013).

Archaeological Significance

The consistent results obtained so far using the U/Th and ^{14}C analysis in the case of sample GN14-17 from mark 1 indicate that these red dots are older than ca. 25,000 yr. This age is coherent with some ^{14}C-AMS dates obtained on charcoals found in the inner galleries, which are attributed to the oldest period of prehistoric occupation (40,000–25,000 yr, cf. Table 3) (Medina-Alcaide and Sanchidrián 2014; Medina-Alcaide et al. 2015). These charcoals were sampled from different Palaeolithic lighting systems (torches, fixed lamps, etc.) that used wood as fuel, as shown by anthracological analyses.

This dating result, which provides a *terminus ante quem* (i.e. a minimum age) for this Palaeolithic mark is the oldest so far obtained in the southern Iberian Peninsula. The only other published ^{14}C dates come from black aurochs in La Pileta Cave, which were dated to 20,130 ±350 BP (GifA 98162; 25,224–23,444 cal BP) (Sanchidrián et al. 2001).

This type of non-figurative marking, related with the oldest phase of Palaeolithic art in this geographical area, can also be found in other caves in southern Spain, such as Ardales, Malalmuerzo, Navarro, Pileta, and Victoria.

CONCLUSIONS AND FUTURE PERSPECTIVES

Two red non-figurative marks representing an ensemble of three red dots (mark 1, GN14-17) and a larger red mark (mark 2, samples GN12-25 and GN12-27) were studied because they are both partially overlain by thin secondary calcareous layers (one layer for mark 1 and two layers in stratigraphic order for mark 2). $^{230}Th/^{234}U$ and ^{14}C crossdating was performed on these three carbonate layers in an attempt to provide a minimum age for the underlying marks. The ages obtained on modern samples were coherent. For sample GN14-17 (mark 1), $^{230}Th/^{234}U$ and ^{14}C age estimations are very close, which suggests the reliability of the two chronometers and

https://doi.org/10.1017/RDC.2017.120 Published online by Cambridge University Press

Table 3 Results of anthropological determinations performed on charcoals from human occupancy of Nerja Cave and ^{14}C ages. They were calibrated using IntCal13 (Reimer et al. 2013). Data from Medina-Alcaide and Sanchidrián (2014) and Medina-Alcaide et al. (2015).

Ref. on map (Figure 1)	Lab nr	Sample type	^{14}C age (BP, 1σ)	Calibrated interval range (cal BP)	Notes
5	Beta-271212	Charcoal	20,980 ± 100	25,555–25,120	Charcoal from the floor
6	Beta-347457	*Pinus* tp. *sylvetris/nigra*	21,900 ± 90	26,235–25,960	Charcoal from the floor
7	Beta-271211	*Pinus* tp. *sylvetris/nigra*	23,800 ± 140	28,075–27,680	Fixed illumination point
8	Beta-298419	*Pinus* cf. *Pinus* tp. *sylvetris/nigra*	23,880 ± 130	28,155–27,730	Charcoal from the floor
9	Beta-277744	Charcoal	24,130 ± 140	28,485–27,860	Charcoal from the floor
10	Beta-306992	*Pinus* cf. *Pinus* tp. *sylvetris/nigra*	29,650 ± 160	34,020–33,600	Fixed illumination point
11	Beta-277745	Indeterminate	35,320 ± 360	40,695–39,035	Fixed illumination point

the low proportion of dead carbon in this part of Nerja Cave for ages of ca. 25,000 yr BP. Considering the large size of the cave (several kilometers in area and two levels of galleries), however, one can expect different proportions of dead carbon from place to place, and further analyses are necessary to date the $CaCO_3$ samples in other galleries. For sample GN12-25 and GN12-17 (mark 2), the very large discrepancy (ca. 30,000 and 10,000 yr, respectively) between the two methods suggests an open system behavior of the secondary carbonate thin deposit and hence an inaccurate age determination. At the archaeological level, the chronological information provided for mark 1 (red dots) indicates that this type of non-figurative sign is older than 25,000 cal BP and that it can be associated with the oldest Palaeolithic occupation of Nerja Cave (39,035–25,555 cal BP).

This paper has reported an attempt to develop an ongoing methodology that could provide an age for non-organic parietal representations. Our results demonstrate that $^{230}Th/^{234}U$ analysis of thin secondary calcareous layers deposited on decorated walls is a very interesting application that needs to be investigated using a rigorous methodological approach: the application of an independent dating method such as ^{14}C dating is mandatory in order to validate the determined ages. Several more sampling campaigns have already been done in Nerja Cave to extend this methodology and to confirm these initial results. They will provide an overview of the possibility of using combined U-Th and ^{14}C dating to understand the chronology of non-organic parietal representations.

ACKNOWLEDGMENTS

The authors wish to thank the IPSL research project (LSCE-CNRS, grant to H Valladas) and *Proyecto General de Investigación Interdisciplinar de la Cueva de Nerja* for their financial support and access to Nerja Cave.

Maria Á Medina-Alcaide has a PhD grant from The Ministry of Education, Culture and Sport of Spain (MECD-FPU) awarded by the University of the Basque Country (UPV/EHU) and the results presented in this paper have been partially funded by the research project of the Spanish Science Ministry HAR2014-53536-P (*La ruta occidental del poblamiento de la Península Ibérica durante el Paleolítico medio y superior*), and the Research Team in Prehistory at the University of the Basque Country (IT-622-13). We thank Nadine Tisnérat-Laborde for her contribution in the preparation of one calcite sample dated by ^{14}C. The two reviewers are also thanked for their valuable remarks. This is LSCE contribution number 6600.

REFERENCES

Aubert M, O'Connor S, McCulloch M, Mortimer G, Watchman A, Richer-La-Fleche M. 2007. Uranium-series dating rock art in East Timor. *Journal of Archaeological Science* 34:991–6.

Aubert M, Brumm A, Ramli M, Sutikna T, Saptomo EW, Hakim B, Morwood MJ, van den Bergh GD, Kinsley L, Dosseto A. 2014. Pleistocene cave art from Sulawesi, Indonesia. *Nature* 514:223–7.

Baker A, Smart PL, Edwards RL, Richards DA. 1993. Annual growth banding in a cave stalagmite. *Nature* 364(6437):518–20.

Bar-Matthews M, Ayalon A, Gilmour M, Matthews A, Hawkesworth CJ. 2003. Sea–land oxygen isotopic relationships from planktonic foraminifera and speleothems in the Eastern Mediterranean region and their implication for paleorainfall during interglacial intervals. *Geochimica et Cosmochimica Acta* 67(17):3181–99.

Bischoff J, García-Diez M, González Morales MR, Sharp W. 2003. Aplicación del método de series de Uranio al grafismo rupestre de estilo paleolítico : el caso de la cavidad de Covalanas (Ramales de la Victoria, Cantabria). *Veleia* 20:143–50.

Borsato A, Quinif Y, Bini A, Dublyansky Y. 2003. Open-system alpine speleothems: implications for U-series dating and paleoclimate reconstructions, *Studi Trentini di Scienze Naturali, Acta Geologica* 80:71–83.

Bruthans J, Schweigstillova J, Jenč P, Churáčková Z, Bezdička P. 2012. ^{14}C and U-series dating of speleothems in the Bohemian Paradise (Czech Republic): retreat rates of sandstone cave walls and implications for cave origin. *Acta Geodyn. Geomater* 9(1):93–108.

Cheng H, Edwards RL, Shen CC, Polyak VJ, Asmerom Y, Woodhead J, Hellstrom J, Wang Y, Kong X, Spötl C, Wang X. 2013. Improvements in ^{230}Th dating, ^{230}Th and ^{234}U half-life values, and U–Th isotopic measurements by multi-collector inductively coupled plasma mass spectrometry. *Earth and Planetary Science Letters* 371:82–91.

Cottereau E, Arnold M, Moreau C, Baqué D, Bavay D, Caffy I, Salomon J. 2007. Artemis, the new ^{14}C AMS at LMC14 in Saclay, France. *Radiocarbon* 49(2):291–9.

Domínguez-Villar D, Carrasco RM, Pedraza J, Cheng H, Edwards RL, Willenbring JK. 2013. Early maximum extent of paleoglaciers from Mediterranean mountains during the last glaciation. *Scientific Reports* 3.

Clottes J. 2012. Datations U-Th, évolution de l'art et Néandertal. *International Newsletter on Rock Art* 64:1–6.

Edwards R, Cheng H, Murrell MT, Goldstein SJ. 1997. Protactinium-231 dating of carbonates by thermal ionization mass spectrometry: implications for Quaternary climate change. *Science* 276(5313):782–6.

Fleitmann D, Matte A. 2009. The speleothem record of climate variability in Southern Arabia. *Comptes Rendus Geoscience* 341(8):633–42.

Fontugne M, Shao Q, Frank N, Thil F, Guidon N, Boeda E. 2013. Cross-dating (Th/U-^{14}C) of calcite covering prehistoric paintings at Serra da Capivara National Park, Piaui, Brazil. *Radiocarbon* 55(2–3):1191–8.

Gascoyne M, Nelson DE. 1983. Growth mechanisms of recent speleothems from Castleguard Cave, Columbia Icefields, Alberta, Canada, inferred from a comparison of uranium-series and carbon-14 age data. *Arctic and Alpine Research* 15(4):537–42.

Genty D, Baker A, Massault M, Proctor C, Pons-Branchu E, Hamelin B. 2001. Dead carbon in stalagmites: carbonate bedrock paleodissolution vs ageing of soil organic matter. Implications for ^{13}C variations in speleothems. *Geochimica et Cosmochimica Acta* 65(20):3443–57.

Gordon D, Smart PL, Ford DC, Andrews JN, Atkinson TC, Rowe PJ, Christopher NS. 1989. Dating of late Pleistocene interglacial and interstadial periods in the United Kingdom from speleothem growth frequency. *Quaternary Research* 31(1):14–26.

Goslar T, Hercman H, Pazdur A. 2000. Comparison of U-series and radiocarbon dates of speleothems. *Radiocarbon* 42(3):403–14.

Griffiths M L, Fohlmeister J, Drysdale RN, Hua Q, Johnson K R, Hellstrom JC, Gagan MK, Zhao JX. 2012. Hydrological control of the dead carbon fraction in a Holocene tropical speleothem. *Quaternary Geochronology* 14:81–93.

Hoffmann DL, Pike AWG, García-Diez M, Pettitt P B, Zilhao J. 2016. Methods for U-series dating of $CaCO_3$ crusts associated with Palaeolithic cave art and application to Iberian sites. *Quaternary Geochronology* 36:104–19.

Holmgren K, Lauritzen SE, Possnert G. 1994. ^{230}Th^{234}U and ^{14}C dating of a late Pleistocene stalagmite in Lobatse II Cave, Botswana. *Quaternary Science Reviews* 13(2):111–9.

Jordá JF, Aura JE. 2008. 70 fechas para una cueva. Revisión crítica de 70 dataciones C14 del Pleistoceno Superior y Holoceno de la Cueva de Nerja (Málaga, Andalucía, España). *Espacio, Tiempo y Forma* I(1):239–56.

Jordá JF, Aura E. 2009. El límite Pleistoceno-Holoceno en el yacimiento arqueológico de la Cueva de Nerja (Málaga, España): nuevas aportaciones cronoestratigráficas y paleoclimáticas. *Geogaceta* 46:95–8.

Kaufman A, Wasserburg G J, Porcelli D, Bar-Matthews M, Ayalon A, Halicz L. 1998. U-Th isotope systematics from the Soreq cave, Israel and climatic correlations. *Earth and Planetary Science Letters* 156(3):141–55.

Medina-Alcaide MA, Sanchidrián JL. 2014. Hacia el lado oscuro: cueva de Nerja a la luz de los nuevos datos. In: Corchón MS, Menéndez M, editors. *Cien años de arte rupestre paleolítico*. Salamanca: Universidad de Salamanca. p 133–41.

Medina-Alcaide MA, Sanchidrián J L, Zapata L. 2015. Lighting the dark: wood charcoal analysis from Cueva de Nerja (Málaga, Spain) as a tool to explore the context of Palaeolithic rock art. *Comptes Rendus Palevol* 14(5):411–22.

Medina-Alcaide MA, Garate DY, Sanchidrián JL. 2017. Painted in red: In search of alternative explanations for European Palaeolithic cave art. *Quaternary International*. https://doi.org/10.1016/j.quaint.2016.08.043.

Mook WG, van der Plicht J. 1999. Reporting ^{14}C activities and concentrations. *Radiocarbon* 41(3):227–39.

Moreno A, Stoll H, Jiménez-Sánchez M, Cacho I, Valero-Garcés B, Ito E, Edwards RL. 2010. A speleothem record of glacial (25–11.6 kyr BP) rapid climatic changes from northern Iberian Peninsula. *Global and Planetary Change* 71(3):218–31.

Noronha AL, Johnson KR, Hu C, Ruan J, Southon JR, Ferguson JE. 2014. Assessing influences on speleothem dead carbon variability over the Holocene: implications for speleothem-based radiocarbon calibration. *Earth and Planetary Science Letters* 394:20–9.

Pike AWG, Gilmour M, Pettitt P, Jacobi R, Ripoll S, Bahn P, Muñoz F. 2005. Verification of the age of the Palaeolithic rock art at Creswell. *Journal of Archaeological Science* 32(11):1649–55.

Pike AWG, Hoffmann DL, García-Diez M, Pettitt PB, Alcolea J, De Balbín R, González-Sainz C, de las Heras C, Lasheras JA, Montes R, Zilhão J. 2012. U-series dating of Paleolithic Art in 11 Caves in Spain. *Science* 336:1409–13. (Supplementary materials: www.sciencemag.org/cgi/content/full/336/6087/1409/DC1)

Plagnes V, Causse C, Fontugne M, Valladas H, Chazine JM, Fage LH. 2003. Cross dating (Th/U-14C) of calcite covering prehistoric paintings in Borneo. *Quaternary Research* 60(2):172–9.

Pons-Branchu E, Bourrillon R, Conkey M, Fontugne M, Fritz C, Gárate D., Quiles A., Rivero O, Sauvet G, Tosello G, Valladas H, White R. 2014a. Uranium-series dating of carbonate formations overlying Paleolithic art: interest and limitations. *Bulletin de la Société préhistorique française* 111(2):211–24.

Pons-Branchu E, Douville E, Roy-Barman Dumont E, Branchu E, Thil F, Frank N, Bordier L, Borst W. 2014b. A geochemical perspective on Parisian urban history based on U-Th dating, laminae counting and yttrium and REE concentrations of recent carbonates in underground aqueducts. *Quaternary Geochronology* 24:44–53.

Pons-Branchu E, Hamelin B, Losson B, Jaillet S, Brulhet J. 2010. Speleothem evidence of warm episodes in northeast France during Marine Oxygen Isotope Stage 3 and implications for permafrost distribution in northern Europe. *Quaternary Research* 74(2):246–51.

Pons-Branchu E, Hillaire-Marcel C, Ghaleb B, Deschamps P, Sinclair D. 2005. Early diagenesis impact on precise U-series dating of Deep-Sea corals. Example of a 100–200 years old Lophelia Pertusa sample from NE Atlantic. *Geochimica et Cosmochimica Acta* 69(20):4865–79.

Quiles A, Fritz C, Medina MA, Pons-Branchu E, Sanchidrián JL, Tosello G, Valladas H. 2014. Chronologies croisées (C-14 et U/Th) pour l'étude de l'art préhistorique dans la grotte de Nerja: méthodologie. In: Medina-Alcaide et al., editors. *Sobre Rocas y Huesos*. Córdoba. ISBN: 978-84-617-2993. p 420–427.

Reimer PJ, Bard E, Bayliss A, Beck W, Blackwell P, Bronk C, Buck C, Cheng H, Edwards L, Friedrich M, Grootes , Guilderson T, Haflidason H, Hajdas I, Hatté C, Heaton T, Hoffmann D, Hogg A, Hughen K, Kaiser F, Kromer B, Manning S, Niu M, Reimer R, Richards D, Scott M, Southon J, Staff R, Turney C, van der Plicht J. 2013. IntCal13 and Marine13 radiocarbon age calibration curves 0–50,000 years cal BP. *Radiocarbon* 55(4):1869–87.

Roy-Barman M, Pons-Branchu E. 2016. Improved U–Th dating of carbonates with high initial 230 Th using stratigraphical and coevality constraints. *Quaternary Geochronology* 32:29–39.

Sanchidrián JL. 1994. *Arte Rupestre de la Cueva de Nerja*. Málaga: Patronato de la Cueva de Nerja: 332 p.

Sanchidrián JL. 1994. Arte paleolítico de la zona meridional de la Península Ibérica. *Complutum* 5:163–95.

Sanchidrián JL. 1997. Propuesta de la secuencia figurativa en la cueva de La Pileta. In: Fullola M, Soler N, editors. *El món mediterrani després del Pleniglacial (18.000-12.000 BP)*. Gerona. p 411–30.

Sanchidrián J, Márquez AM, Valladas H, Tisnerat N. 2001. Dates directes pour l'art rupestre d'Andalousie (Espagne). *International Newsletter on Rock Art* 29:15–19.

Sanchidrián JL, Valladas H, Medina-Alcaide MÁ, Pons-Branchu E, Quiles A. 2017. New perspectives for ^{14}C dating of parietal markings using $CaCO_3$ thin layers: an example in Nerja cave (Spain). *Journal of Archaeological Science Reports* 12:74–80.

Shao QF, Pons-Branchu E, Zhu QP, Wang W, Valladas H, Fontugne M. 2017. High precision U/Th dating of the rock paintings at Mt. Huashan, Guangxi, southern China. *Quaternary Research* 88(1):1–13.

Siddall M, Rohling EJ, Thompson WG, Waelbroeck C. 2008. Marine isotope stage 3 sea level fluctuations: data synthesis and new outlook. *Reviews of Geophysics* 46(4):RG4003.

Tisnérat-Laborde N, Poupeau JJ, Tannau JF, Paterne M. 2001. Development of a semi-automated system for routine preparation of carbonate samples. *Radiocarbon* 43(2A):299–304.

Tuccimei P, van Strydonck M, Ginés A, Soligo M, Villa IM, Fornós JJ. 2011. Comparison of ^{14}C and U-Th ages of two Holocene phreatic overgrowths on speleothems from Mallorca (Western Mediterranean): environmental implications. *International Journal of Speleology* 40(1):1.